JOURNAL OF Materials CHEMISTRY

New polycyclic aromatic hydrocarbon dopants for red organic electroluminescent devices

B. X. Mi,[a] Z. Q. Gao,[a] M. W. Liu,[a] K. Y. Chan,[b] H. L. Kwong,[b] N. B. Wong,[a,b] C. S. Lee,[a] L. S. Hung[a] and S. T. Lee*[a]

[a]*Center of Super-Diamond & Advanced Films (COSDAF) and Department of Physics & Materials Science, City University of Hong Kong, Hong Kong SAR, China. E-mail: apannale@cityu.edu.hk; Fax: 852-27887830*
[b]*Department of Biology & Chemistry, City University of Hong Kong, Hong Kong SAR, China*

Received 7th November 2001, Accepted 12th February 2002
First published as an Advance Article on the web 18th March 2002

Two new anthracene derivatives with red emission have been synthesized. The materials were characterized with photoluminescence spectroscopy, and showed emission peaking at over 600 nm. Organic light-emitting devices were fabricated by using these derivatives as dopants. The devices have a maximum efficiency of 0.6 cd A^{-1} and an emission peak at 617 nm. The results of color tuning and fluorescent yield enhancement for anthracene derivatives are presented.

Introduction

Organic light-emitting diodes (OLEDs) have been considered as the next generation of flat panel displays (FPD) because of their considerable merits, such as light weight, thin structure, wide viewing angle, high contrast ratio, low power consumption, video-rate response time, and availability of full color. The new technology has stimulated intensive research activities during the past decade after the report by Tang and VanSlyke.[1] Recently, dot matrix OLED panels with blue and green colors became commercially available for automotive entertainment, and a full color QVGA (quarter video graphics array, *i.e.* 320 dots × 240 dots) panel was also demonstrated.[2] In spite of the fast developments of OLEDs, red emission from OLEDs with high color purity and good stability is badly needed.[3] Red materials for OLEDs with a high fluorescent quantum yield are not as common as blue or green materials. Up to now, several organic compounds with red emission have been reported, such as pyran-containing compounds,[4] porphyrin compounds,[5] and europium metal complexes.[6] Because of the instability of rare earth metal complexes during thermal deposition,[7] no europium metal complexes show a practical operation lifetime even though they have a sharp emission peak with high color purity. The most promising red dopant among the porphyrin compounds is platinum octaethylporphyrin (PtOEP)[8] with its phosphorescent quantum yield of about 0.5. Although high-efficiency phosphorescent emission using tris(8-quinolinolato)aluminium (AlQ_3) doped with PtOEP has been achieved at a low current density, the brightness and chromaticity of this device for practical operation are not acceptable. Pyran-containing compounds, such as 4-dicyanomethylene-2-methyl-6-(*p*-dimethylaminostyryl)-4*H*-pyran (DCM),[9] 4-(dicyanomethylene)-2-methyl-6-(1,1,7,7-tetramethyljulolidin-9-yl)-4*H*-pyran (DCJT),[10] and 4-(dicyanomethylene)-2-*tert*-butyl-6-(1,1,7,7-tetramethyljulolidin-9-yl)-4*H*-pyran (DCJTB)†[4] have been widely used for dopant emitters in red OLEDs. These dyes possess a highly concentration dependent emission. A desirable red color (CIE: $x = 0.64$, $y = 0.36$) can only be obtained at high concentration, however, which dramatically reduces luminance efficiencies. In an active matrix (AM)-OLED full color display, a significant portion of the operating power is consumed by red channels.[11] In order to reduce the power consumption of OLED panels, synthesis of red materials with high efficiency and color purity remains challenging.

The emission wavelength of a fluorescent dye depends on the energy gap between the highest occupied molecular orbital (HOMO) and lowest unoccupied molecular orbital (LUMO) of the molecule. Materials with red emission generally have a narrow energy gap. It is well known that the energy gap of polycyclic aromatic hydrocarbon (PAH) compounds depends on the conjugation length of the molecules: the longer the conjugation length, the lower the energy gap of the PAH compounds.[12] On the other hand, many PAH compounds have a very high fluorescent quantum yield, and stable OLEDs have been fabricated based on these PAH compounds, such as rubrene[13] and perylene.[14] It is believed that OLEDs based on PAH compounds should possess stable operating properties. But these useful PAH compounds emit light mainly in the blue and yellow regions with only a few PAH compounds reported to have emission above 600 nm. Moreover, PAH compounds with more fused carbon rings have a high sublimation temperature. This limits the application of red-emission PAH compounds in OLEDs.

The conjugation length of a fluorescent PAH compound can be enlarged to give a red shift in two ways: one way is to increase the fused benzene rings linearly such as naphthalene, anthracene, tetracene and pentacene. The other way is to add benzene rings or fused benzene rings in two dimensions to form PAH *peri*-compounds. In this work, we attempted to obtain red-emitting PAH compounds based on the anthracene skeleton, which can be modified to form PAH *peri*-compounds.

Experimental

Materials

All the starting materials and solvents for synthesis of red materials were purchased from Aldrich or Acros companies. Tetrahydrofuran (THF) was dried by refluxing and distilling with sodium and monitored using benzophenone. AlQ_3, *N*,*N*′-bis (1-naphthyl)-*N*,*N*′-diphenyl-1,1′-biphenyl-4,4′-diamine (NPB), and a trimer of *N*-arylbenzimidazoles (TPBI) were synthesized in our laboratory. AlQ_3 was purified further by

†The IUPAC name for julolidine is 2,3,6,7-tetrahydro-1*H*,5*H*-pyrido[3,2,1-*ij*]quinoline.

train sublimation under nitrogen several times. Patterned indium tin oxide (ITO) coated glasses with a sheet resistance of 30 Ω/□ were used as substrates.

Apparatus

Proton NMR (^{1}H, 300 MHz) spectra of samples in solutions were recorded at room temperature on a Varian instrument. Photoluminescence (PL) and absorption spectra were measured with a Perkin-Elmer LS50 fluorescence spectrophotometer and a Perkin-Elmer Lambda 2S UV–Visible spectrophotometer respectively in dilute solutions of 1×10^{-5} M. OLEDs were fabricated using a modified Edward AUTO 306 vacuum chamber at a base pressure of 5×10^{-6} mbar. All the materials were deposited in one pump-down. Two shadow masks were used to define the deposition area, respectively, for organic and metal layers. The current–voltage–luminance characteristics and EL spectra of the devices were measured with a computer-controlled DC power supply and a Spectrascan PR650 photometer at room temperature. The emission area of the devices is 0.1 cm^2, defined by the overlapping area of the anode and cathode.

Synthesis of red dopant materials

Two red dopant materials, tetrabenzo[*de*,*hi*,*op*,*st*]pentacene (DpNA) and 7-(9-anthryl)dibenzo[*a*,*o*]perylene (pAAA), with the chemical structures shown in Fig. 1, were synthesized according to the procedure described in the literature.[15] In the synthesis of DpNA, 1,5-dichloroanthraquinone and 1-bromonaphthalene were used as starting materials. First, the 1,5-dichloroanthraquinone was condensed with 1-naphthylmagnesium bromide in dry THF, which was freshly prepared from 1-bromonaphthalene and magnesium turnings. Second, the resulting diol was reduced with hydrogen iodide to the corresponding anthracene. Finally, by heating the product from step two with (1 mol : 30 mol) potassium hydroxide in quinoline solution, DpNA was obtained. This crude product was purified by recrystallization in xylene, then by sublimation under vacuum. Melting point: 333–334 °C; ^{1}H NMR (benzene-d_6, 300 MHz) δ: 8.52(d, 2 H), 8.12(d, 2 H), 8.06(d, 2 H), 7.07(d, 2 H), 7.55(d, 2 H), 7.48(d, 2 H), 7.40(s, 2 H), 7.30(m, 1 H), 7.22(m, 3 H); calc. for $C_{34}H_{18}$: C: 95.7%, H: 4.2%, found: C: 95.3%, H: 4.3%; IR (KBr disk, ν/cm^{-1}): 3047 (s), 1599 (w), 1570 (w), 1500 (w), 1420 (w), 1383 (w), 1345 (w), 836 (s), 795 (s), 775 (s), 760 (s), 748 (s); UV–vis [λ/nm (ε/cm^{-1} M^{-1})]: CH_2Cl_2, 623 (12930), 577 (7510), 290 (11290).

In the synthesis of pAAA, a lithium reagent was used instead of magnesium turnings. This was due to the thermal instability of the starting material 9-bromoanthracene. In a 100 ml flask, 3.2 g (12.4 mmol) 9-bromoanthracene and 8 ml dry THF were introduced. The temperature was lowered to −78 °C. 8.9 ml (14.2 mmol) of 1.6 M n-BuLi hexane solution was added dropwise *via* an addition funnel. The dark orange suspension obtained was stirred at this temperature for half an hour. Then 1.5 g (6.2 mmol) 1-chloro-9,10-anthraquinone in 30 ml dry THF was added *via* an addition funnel. The reaction mixture was allowed to warm up to room temperature at constant stirring for 1 hour, and was then hydrolyzed with 30 ml 2 M Na_2CO_3 under N_2 for another hour. The organic layer was separated and the water layer was extracted three times with THF. The solvent was removed, and the organic layers were collected, combined with the first separated organic layer, and washed with ether to obtain a pale yellow product, 1-chloro-9,10-di(9′-anthryl)-9,10-dihydroanthracene-9,10-diol. Then, similar to the preparation of DpNA, the resulting diol was reduced with hydrogen iodide to the corresponding anthracene. By heating the corresponding anthracene from step two with potassium hydroxide, the pAAA crude product was obtained. This dark violet solid was very unstable in solution, due to its sensitivity to light and oxygen. However, it could be purified by column chromatography using (1 : 3) benzene and petroleum ether as carrier. Melting point: 156–160; ^{1}H NMR (chloroform-d, 300 MHz) δ: 8.72(s, 1 H), 8.46(s, 1 H), 8.25(d, 1 H), 8.18(d, 3 H), 8.06(dd, 2 H), 7.68(dd, 2 H), 7.48(m, 2 H), 7.30(dd, 6 H), 7.22(d, 2 H), 7.13(dd, 4 H); MS: *m*/*z* 528.1 (M$^+$); calc. for $C_{42}H_{24}$: C: 95.4%, H: 4.5%, found: C: 96.7%, H: 4.3%; IR (KBr disk, ν/cm^{-1}): 3048 (s), 1442 (w), 1307 (w), 883 (m), 842 (m), 798 (m), 759 (s), 733 (s); UV–vis [λ/nm (ε/cm^{-1} M^{-1})]: CH_2Cl_2, 572 (12050), 532 (7670), 297 (18840).

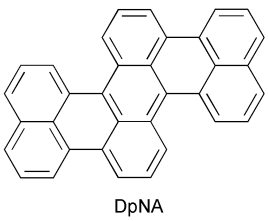

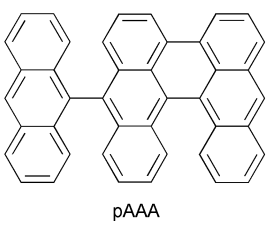

Fig. 1 Chemical structures of the red dopants reported.

Preparation of OLED devices

The chemical structures of the organic materials other than the red dopants used in the device fabrication are shown in Fig. 2. Several device configurations were utilized in order to evaluate the performance of the red materials. The ITO glass substrate

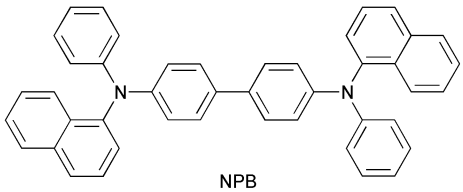

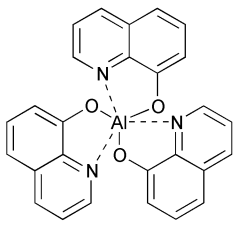

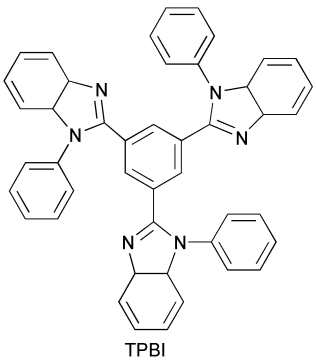

Fig. 2 Chemical structure of organic materials used in the study other than the red dopants.

was cleaned with detergents and deionized water, and dried in an oven for about two hours. Then, it was treated with UV–ozone for 25 minutes prior to loading into a deposition chamber. Organic materials were sequentially deposited onto the ITO substrate at a pressure around 1.0×10^{-5} mbar to form the desired device configurations. The pressure during metal deposition was below 9.0×10^{-6} mbar.

Results and discussion

1. DpNA devices

Fig. 3 shows the absorption spectra of a DpNA film and a DpNA solution in toluene, and the PL spectrum is shown in the inset. The PL emission is around 647 nm in toluene solution. Due to the rigid structure of this material, the overlap of the absorption and emission spectra is very marked.[16] The PL yield is low because the luminance suffers severely from self-absorption in this compound which can act as an inner filter.[16] It may also be attributed to a small difference in energy levels between the excited singlet state and triplet state of DpNA, as observed in anthracene solids.[17] Intersystem crossing could result in internal quenching of excited singlet states.[16] The first absorption peaks of the DpNA film and solution are 667 nm and 628 nm respectively. The absorption peak of the DpNA film shifts to red by 40 nm as compared to the DpNA solution, and the width of the absorption peak broadens, implying strong intermolecular interactions in DpNA. This is expected from the planar structure of DpNA, which causes concentration quenching.[16] It is clear from the results that this material can only be used as a dopant in OLEDs.

Because the absorption peak of DpNA in diluted solution is around 628 nm, it is very difficult to find a host material to match the resonance energy transfer conditions. We used different host materials to optimise the performance of OLED devices. The best result was obtained with a device of structure ITO/NPB–1% DpNA (70 nm)/TPBI–1% DpNA (50 nm)/Mg–Ag (200 nm). The EL and current–voltage characteristics of this device are shown in Fig. 4. The maximum luminance is only 22 cd m^{-2}, and the emission of TPBI cannot be completely extinguished. The poor performance is attributed to both the planar structure of DpNA and the poor energy matching between the host and the dopant.

We tried to modify the structure of DpNA to enhance the PL yield[18] by breaking down one *peri*-bond of DpNA, and a compound with a very high PL yield was obtained. However, the emission shifted to green because of the reduction in the conjugation length. Therefore, we designed another PAH compound, pAAA.

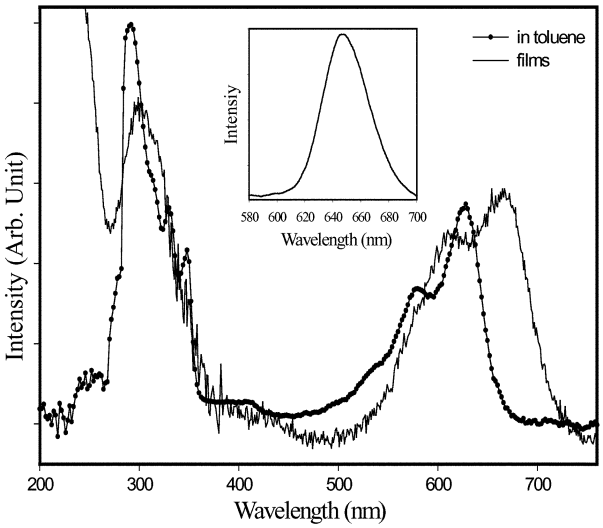

Fig. 3 Absorption spectra of the DpNA film and solution (in toluene), and the PL spectrum (inset).

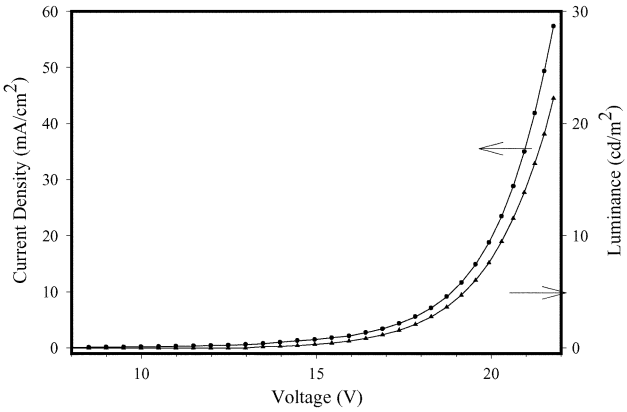

Fig. 4 EL and current–voltage characteristics of a device with the configuration ITO/NPB–1% DpNA (70 nm)/TPBI–1% DpNA (50 nm)/Mg–Ag (200 nm).

2. pAAA devices

Fig. 5 shows the absorption and PL spectra of pAAA in dilute solution. The PL peak of pAAA is at 608 nm. The chemical structure of this compound is not as rigid as DpNA. It has a rotatable anthryl group. For this reason, the Stokes shift of pAAA is larger than that of DpNA. The reduced self-absorption of pAAA molecules can increase the PL quantum efficiency of this compound compared to DpNA. Furthermore, similar to DpNA, the PL quantum efficiency can also be improved by decreasing the intersystem crossing from the excited singlet to excited triplet because of the rotatable anthryl substituted group.[17] The width of the PL peak is only 40 nm. This narrow emission is very attractive because high color purity can be expected using this material. The first absorption peak is around 568 nm, and the second absorption peak is around 530 nm. The vibronic spacing of 1262 cm^{-1} between 568 and 530 nm may correspond to a number of C–H aromatic in-plane deformation bands.[19] The fluorescence quantum yield (Qy) is 0.1 measured with Rhodamine B (Qy = 0.66) as standard, using non-degassed spectrophotometric grade CH_2Cl_2 as solvent. It should be noted that the fluorescence of aromatic molecules is strongly oxygen quenched[20] and this will dramatically reduce the measured value. The red emission can be clearly seen under 365 nm UV lamp excitation. Also, in Fig. 5, the EL spectrum of AlQ_3 is shown. There were three vibration peaks in the pAAA absorption spectrum, of which the second and the third ones were fully overlapped by the

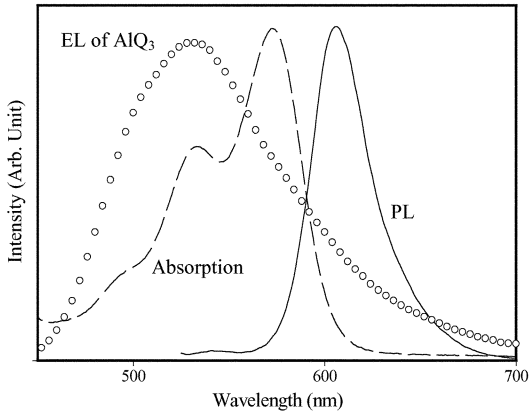

Fig. 5 Absorption and PL spectra of pAAA in dilute solution, and AlQ_3 electroluminescence of a device with the configuration ITO/NPB (70 nm)/AlQ_3 (70 nm)/Mg–Ag(200 nm).

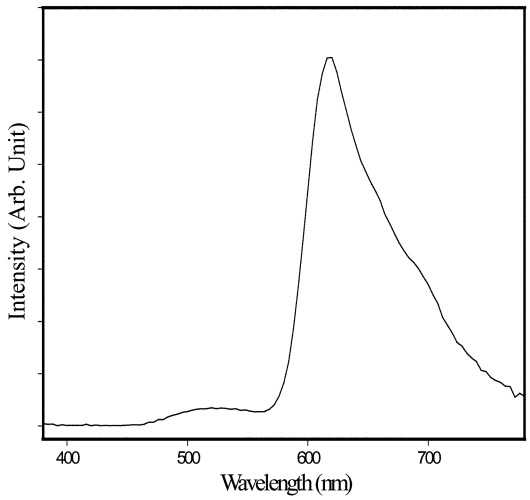

Fig. 6 The EL spectrum of a device with the configuration ITO/NPB (70 nm)/AlQ_3–2% pAAA (35 nm)/AlQ_3 (35 nm)/Mg–Ag(200 nm).

emission spectrum of AlQ_3 emission. However the strongest peak of pAAA absorption did not overlap much with the emission of AlQ_3. As a result, the energy transfer from AlQ_3 to pAAA is not efficient and the AlQ_3 emission cannot be totally suppressed in the presence of pAAA, as shown in Fig. 6.

OLEDs with the structure ITO/NPB (70 nm)/AlQ_3–2% pAAA (35 nm)/AlQ_3 (35 nm)/Mg–Ag (200 nm) were prepared. The EL spectrum of the devices in Fig. 6 reveals an emission peak at about 616 nm. The CIE coordinates are $x = 0.625$, $y = 0.358$. It can be seen that the emission of the device is broader than the PL of the pAAA. The intensity of this peak increases with increasing dopant concentrations of the device. This might be attributed to the dimer or trimer emission of pAAA molecules. It is evident from Fig. 6 that the AlQ_3 emission cannot be completely converted to pAAA emission, indicating that a better host material is needed in order to achieve higher efficiency and purer red emission.

The plot of luminance efficiency *vs.* current density is shown in Fig. 7. The efficiency is almost constant over a large range of current density with a maximum value of about 0.6 cd A^{-1}. The constant efficiency will facilitate the design of driving circuits in OLED displays.

Conclusions

Two red materials for OLEDs were designed and synthesized. OLEDs were fabricated using these red materials as dopants. The devices with pAAA dopants can achieve a current efficiency 0.6 cd A^{-1} with CIE coordinates of $x = 0.625$, $y = 0.358$.

Acknowledgement

This work is supported by the Research Grants Council of Hong Kong SAR *via* a grant [no. Cityu 1/98c (8730009)].

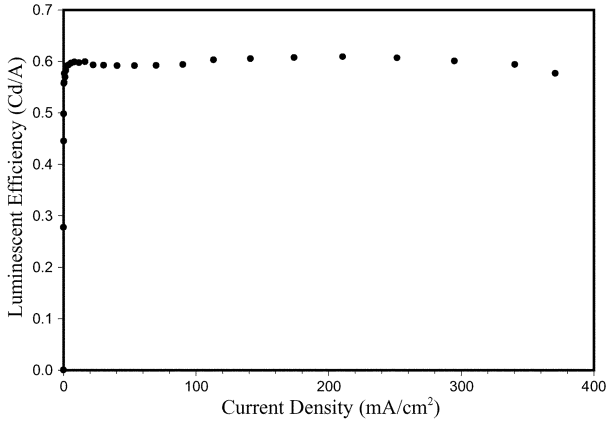

Fig. 7 Luminance efficiency of a device with the configuration ITO/NPB (70 nm)/AlQ_3–2% pAAA (35 nm)/AlQ_3 (35 nm)/Mg–Ag(200 nm).

References

1 C. W. Tang and S. A. VanSlyke, *Appl. Phys. Lett.*, 1987, **51**, 913.
2 Y. Fukuda, T. Watanabe, T. Wakimoto, S. Miyaguchi and M. Tsuchida, *Synth. Met.*, 2000, **111–112**, 1.
3 C. H. Chen, J. Shi and C. W. Tang, *Macromol. Symp.*, 1997, **125**, 1.
4 C. H. Chen, C. W. Tang, J. Shi and K. P. Klubek, *Thin Solid Films*, 2000, **363**, 327.
5 P. E. Burrows, S. R. Forrest, S. P. Sibley and M. E. Thompson, *Appl. Phys. Lett.*, 1996, **69**, 2959.
6 J. Kido, H. Hayase, K. Hongawa, K. Nagai and K. Okuyama, *Appl. Phys. Lett.*, 1994, **65**, 2124.
7 J. Kido, W. Ikeda, M. Kimura and K. Nagai, *Jpn. J. Appl. Phys.*, 1996, **35**, L394.
8 M. A. Baldo, D. F. O'Brien, Y. You, A. Shoustikov, M. Sibley, M. E. Thompson and S. R. Forrest, *Nature*, 1998, **395**, 151.
9 C. W. Tang, S. A. VanSlyke and C. H. Chen, *J. Appl. Phys.*, 1989, **65**, 3610.
10 C. W. Tang, *Dig. Soc. Information Display Int. Symp.*, 1996, **27**, 181.
11 G. Rajeswaran, M. Itoh, M. Boroson, S. Barry, T. K. Hatwar, K. B. Kahen, K. Yoneda, R. Yokoyama, T. Yamada, N. Komiya, H. Kanno and H. Takahashi, SID 00 Digest, 40.1, 2000.
12 B. M. Krasovitskii and B. M. Bolotin, *Organic Luminescent Materials*, translated by V. G. Vopian, VCH, Weinheim, 1988.
13 M. Arai, K. Nakaya, O. Onitsuka, T. Inoue, M. Codama, M. Tanaka and H. Tanabe, *Synth. Met.*, 1997, **91**, 21.
14 S. A. VanSlyke, *US Patent*5 151 629, 1992.
15 E. Clar, W. Kelly and J. W. Wright, *J. Chem. Soc.*, 1954, 1108.
16 J. B. Birks, *Photophysics of Aromatic Molecules*, Wiley, London, New York, 1970.
17 J. Malkin, *Photophysical and Photochemical properties of aromatic compounds*, CRC Press, Boca Raton, FL, 1992.
18 B. X. Mi, Z. Q. Gao, C. S. Lee, H. L. Kwong, N. B. Wang and S. T. Lee, *J. Mater. Chem.*, 2001, **11**, 2244.
19 G. Socrates, *Infrared Characteristic Group Frequencies: Tables and Charts*, Wiley, Chichester, 2nd edition, 1994, p. 122.
20 J. N. Demas and G. A. Crosby, *J. Phys. Chem.*, 1971, **75**, 991.